Available online at www.sciencedirect.com

ScienceDirect

journal homepage: www.elsevier.com/locate/he

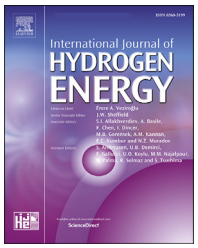

Hydrogen storage and electrochemical properties of annealed low-Co AB_5 type intermetallic compounds

A.N. Kazakov [a,*], D.V. Blinov [a,b], V. Yu Bodikov [a,b], S.V. Mitrokhin [c], A.A. Volodin [a,d]

[a] Joint Institute for High Temperatures, Moscow, Russia
[b] National Research University "Moscow Power Engineering Institute", Moscow, Russia
[c] Lomonosov Moscow State University, Moscow, Russia
[d] Institute of Problems of Chemical Physics of Russian Academy of Sciences, Russia

HIGHLIGHTS

- Low Co AB_5 type alloys were studied as anode materials.
- The maximum discharge capacity 321.1 mA h/g at 100 mA/g for La alloy.
- The hydrogen diffusion coefficient at charging is measured by PITT.
- High cycling retention of 92.2% after 100 cycles at 1C for Nd alloy.

ARTICLE INFO

Article history:
Received 19 March 2020
Received in revised form
1 December 2020
Accepted 10 December 2020
Available online 30 December 2020

Keywords:
Metal hydride
Hydrogen storage
Electrochemical properties
Hydrogen capacity
Hydrogen diffusion

ABSTRACT

The structure, hydrogen storage and electrochemical properties of annealed low-Co AB_5-type intermetallic compounds have been investigated. La-alloy, Nd-alloy and Cr-alloy are used to represent $La_{0.8}Ce_{0.2}Ni_4Co_{0.4}Mn_{0.3}Al_{0.3}$, $La_{0.6}Ce_{0.2}Nd_{0.2}Ni_4Co_{0.4}Mn_{0.3}Al_{0.3}$ and $La_{0.6}Ce_{0.2}Nd_{0.2}Ni_{3.8}Co_{0.4}Mn_{0.3}Al_{0.3}Cr_{0.2}$, respectively. The XRD results indicated that annealed samples are all single-phase alloys with $CaCu_5$ type structure. The maximum of both hydrogen content and discharge capacity is obtained for La-alloy 1.23 wt%H_2 and 321.1 mA h/g, respectively. All the investigated alloys are quiet stable with ΔH of hydrogen desorption about 36–38 kJ/mol H_2. Cycle life of alloy electrode has been improved by partial substitution of La for Nd and Ni for Cr. The highest capacity retention of 92.2% after 100 charge/discharge cycles at 1C has been observed for Nd-alloy. The hydrogen diffusion coefficient measured by PITT is higher at the start of charging process and dramatically reduces by 2–3 order of magnitude with saturation of β-hydride. The highest value 6.9×10^{-13} cm^2/s is observed for La alloy at 100% SOC. Partial substitution La for Nd and Cr for Ni in low-Co AB_5 metal hydride alloys slightly reduces maximum discharge capacity, HRD performance and hydrogen diffusion kinetics. Low-Co alloys show good overall electrochemical properties compared to high-Co alloys and might be perspective materials for various electrochemical applications.

* *Corresponding author.*
E-mail address: kazakoffalex09@gmail.com (A.N. Kazakov).
https://doi.org/10.1016/j.ijhydene.2020.12.071

Introduction

Since early 1970s multicomponent metal hydride materials are extensively investigated for their use in stationary and portable hydrogen storage [1,2], metal hydride hydrogen compresssion [3], thermal energy storage [4] and Ni-MH batteries [5,6]. Among all the applications, Ni-MH batteries have achieved the greatest commercial success and widespread use. In early 1990s Ni-MH batteries based on AB_5-type intermetallic compounds as anode have replaced environmentally hazardous Ni-Cd batteries.

Another electrochemical application, where metal hydrides can be used, is alkaline metal hydride-air fuel cells (MH FC) [7–9]. The MH FC is a device with built-in charge storage, which can operate reversibly as an electrolyzer and hydrogen is absorbed by the metal hydride alloy, i.e.as unitized regenerative fuel cells. Storing charge in or near a fuel cell's electrode of MH FC would speed up the device's response, allow it to be 'recharged' without stopping and to live longer than conventional fuel cells, although the power densities reported were low, the cells stored voltage for minutes or hours [10]. For a MH FC the measured maximum power output was 34 mW/cm^2 (oxygen) [8]. MH electrode has a good catalytic activity for hydrogen and long-term electrochemical stability at a current load of 40–50 mA/cm^2 at 55 °C and lab-size rechargeable metal hydride-air cell with charge efficiency about 90% and specific energy density about 95 Wh/kg was developed [7,11]. A Metal Hydride Fuel Cell was demonstrated in 320 W stacks and 500 W systems by Ovonic Fuel Cell Company [12]. A novel electrochemical reactor for hydrogen production and power generation is proposed based on a fuel cell/battery system with the energy conversion efficiencies of hydrogen production and of the complete hydrogen production/power generation process at a current density of 37.0 mA/cm^2 were 98.3% and 79.6%, respectively [13].

According to electrochemical applications, the most important properties of metal hydride materials are activation performance, discharge capacity, high-rate dischargeability, cyclic stability. Metal hydride (MH) alloys have to meet the following requirements [14–19]:

- High reversible hydrogen storage capacity (>1% mass);
- Rapid initial activation and high catalytic activity;
- Good corrosion resistance in alkaline electrolyte and mechanical stability;
- Fast charge/discharge kinetics and long cycle life;
- Charge/discharge at high current densities and resistance to overcharge/overdischarge;
- Wide range of operating temperatures;
- Environmental friendliness and low-cost production.

The hydrogen absorbing intermetallic compounds (IMC) used for electrochemical applications can be represented by a general formula $A_mB_nH_x$, where A is a hydride forming metal (La, Ce, Mm, Ti, Zr, V, Mg), and metal B does not interact with hydrogen under normal conditions (Ni, Co, Fe, Mn, Cr, Al and others) [2]. Depending on the metal A to metal B ratio, the IMCs can be classified in several basic types: AB_5, AB_2, $AB_{3\text{-}3.5}$, AB, A_2B, Ti-, V-based solid solutions [5].

Despite the great efforts to develop new hydrogen absorbing materials with enhanced working characteristics [5,14,20–27] AB_5 type alloys still stay the most popular materials due to their high surface catalytic activity, easy activation and good cycle stability. The main representative of AB_5 alloys is $LaNi_5$ with $CaCu_5$ hexagonal structure. The hydrogen storage capacity of $LaNi_5H_{6.6}$ hydride is ~1.4 mass% [28–31], which corresponds to a theoretical electrochemical capacity of 372 mA h/g. However, the high equilibrium hydrogen sorption/desorption pressure and the dissolution of La in alkaline electrolytes greatly decrease the electrochemical properties of the alloy. Partial substitution La by mishmetal Mm (mixture of rare earth metals La, Ce, Nd, Pr) and Ni by Co, Mn, Al, Fe, Cr, Sn, etc. allow to reach higher electrochemical capacities and kinetics [14,32–36]. Most popular commercially available alloy is $MmNi_{3.55}Co_{0.75}Mn_{0.4}Al_{0.3}$, where Mm = $La_{0.62}Ce_{0.27}Nd_{0.08}Pr_{0.03}$ [37]. The rare earth elements La, Ce, Pr and Nd are hydride forming metals and primarily provide H_2 absorption, Ni provides catalytic activity for redox reaction, Co, Mn and Sn provide surface activity, and Al and Fe provide corrosion resistance [14,16]. Commercial AB_5 hydrogen storage alloys have reached a reversible discharge capacity of 320–350 mA h/g.

The increase of Al content in $LaNi_{4.4\text{-}x}Co_{0.3}Mn_{0.3}Al_x$ (x = 0–0.3) alloys improves cycle stability and maximum discharge capacity and decreases self-discharge rate. Capacity loss during self-discharge after the complete storage time of 4 days decreased from 17.14% for Al-free alloy (x = 0) to 12.47% for high Al-substituted alloy (x = 0.3) [38]. Partial substitution Ni for Mn increases maximum discharge capacity, cyclic stability [39] and improves low temperature electrochemical performances [32]. Substitution by Fe to multicomponent AB_5 alloys significantly improves cycle stability, corrosion resistance, but lowers discharge capacity and high rate dichargeability [35,40]. Cobalt is a key element to maintain cycle life of metal hydride electrode materials, but the use of Co greatly increases total cost of metal hydride alloy. One of the key factors to increase market competitiveness of Ni-MH batteries is a cost reduction of metal hydride alloys. Partial or complete substitution of Co by cheaper metals Fe, Mn, Al, etc. to reduce material cost were widely investigated [34,35,41–43]. Unfortunately, low-Co and Co-free alloys show lower discharge capacity and cycle life in comparison with usual Co containing (up to 10 at%) alloys. A number of works [44–47] were conducted to investigate partial substitution of conventional components such Ni, Co, Mn, Cu by commercially available ferrovanadium $V_{0.81}Fe_{0.19}$ on electrochemical properties of $AB_{5\text{-}x}(V_{0.81}Fe_{0.19})_x$ (where x = 0–0.2). Alloys with $V_{0.81}Fe_{0.19}$ at concentration x = 0.05–0.1 reached discharge capacity of 310–330 mA h/g and significantly increased cyclic stability.

Along with element substitution, annealing treatment and chemical surface treatment are generally used to improve electrochemical properties of the alloys [33,48–51]. Duplex hot-alkali treatment with reducing agents N_2H_4, NaH_2PO_2, $NaBH_4$ of $MmNi_{3.7}Co_{0.7}Mn_{0.3}Al_{0.3}$ alloy surface significantly enhanced cyclic stability, high rate dischargeability and low temperature characteristics [33]. In addition, a significant increase in high rate dischargeability after alkaline treatment of metal hydride samples was noted in Ref. [49,50]. Annealing

treatment at different temperatures allowed to increase maximum discharge capacity and cyclic stability [48,51].

In order to increase cost-effectiveness of metal hydride materials, two approaches were taken to reduce the raw material cost: elimination/reduction of Pr and Nd in the A-site and reduction of Co in the B-site in comparison with commercially available Mm based alloy [37]. Three different AB_5 type alloys based on $La_{0.8}Ce_{0.2}Ni_4Co_{0.4}Mn_{0.3}Al_{0.3}$ composition are investigated in detail to determine crystal structure, gas phase hydrogen sorption properties and electrochemical characteristics. The obtained results are discussed in comparison with available reference data.

Experimental procedure

AB_5 alloys with nominal compositions $La_{0.8}Ce_{0.2}Ni_4Co_{0.4}Mn_{0.3}Al_{0.3}$ (La-alloy), $La_{0.6}Ce_{0.2}Nd_{0.2}Ni_4Co_{0.4}Mn_{0.3}Al_{0.3}$ (Nd-alloy) and $La_{0.6}Ce_{0.2}Nd_{0.2}Ni_{3.8}Co_{0.4}Mn_{0.3}Al_{0.3}Cr_{0.2}$ (Cr-alloy) are prepared by argon arc melting of pure constituent elements. At first, stoichiometric amounts of metals are joined together at a low voltage and are melt later at least three times at full power. As cast alloys are annealed at 1223 K for 24 h and are quenched into ice water after the annealing. The crystal structure and qualitative compositions of the annealed alloys are defined by means of X-ray diffractometry (Bruker's D8 ADVANCE diffractometer). Samples for XRD analysis are prepared by mechanical grinding to a fine powder. The step size was 0.02° and the exposition time was 1 s. The 2θ angles scanned were in the range from 15 to 80. Processing of diffraction patterns was performed using Jana 2006 and Crystal Impact Match software using JCPDS PDF-2 Data Base.

Hydrogen sorption properties as Pressure-Concentration-Temperature (PCT) of the alloys are measured by volumetric technique in a Sievert's type apparatus. Samples mass of about 5 g are cleaned from surface oxide films and placed in a working autoclave. The volume of working autoclave is evacuated to a residual pressure 1 Pa, then it is connected to hydrogen containing buffer tank. Activation procedure includes evacuation at 473 K for 1 h and following three cycles of hydrogen absorption at 5 MPa and desorption at room temperature. The hydrogen desorption isotherms are measured after the alloy's activation. PCT curves of hydrogen desorption are measured in a temperature range 295–333 K.

Metal hydride electrodes are prepared from powder fraction with a particle size of 40–60 μm and the average particle size assumed to be 50 μm. Pellet type electrode samples consist of 20 wt% of MH powder and 80 wt% of carbonyl Ni and have total mass of 0.5 g. The pellet electrodes with diameter of 10 mm and thickness about 1 mm are fabricated by cold-pressing under a pressure of 25 MPa for 3 min. Then fabricated pellet is pressed between two Ni foam plates connected to the current collector.

Electrochemical properties are investigated at room temperature using an open three-electrode cell with a 6 M aqueous KOH electrolyte solution. Hg/HgO electrode is used as a reference electrode. Sintered $Ni(OH)_2$/NiOOH plate is used as a counter electrode and got a much higher capacity as compared to the working electrode. The experiments are performed using a multichannel potentiostat P-20X8 from ElectroChemical Instruments. MH electrode is immersed to alkaline solution for 2 h to get fully wetted and then it is activated for 10 cycles by fully charging at a current density of 100 mA/g for 4 h and then discharged at 100 mA/g to the cut-off voltage of 0.6 V. High-rate dischargeability performance of metal hydride electrodes are measured in a current density range 100–1000 mA/g. Cyclic stability are measured at current density 300 mA/g (1C) during 100 cycles. Hydrogen diffusion was measured by potentiostatic intermittent titration technique (PITT). The method PITT consists in sequentially applying a step of the potential ΔE -20 mV in the range of −0.84 to −0.96 V, followed by fixing the current change in time until the minimum current value is reached at each step. This technique successfully applied to the conductive polymers and lithium intercalation materials [52–54], RE-Mg-Ni alloys [24,55] and La-doped AB_2 alloy [56]. Measurements are performed using different samples to exclude the influence of charge/discharge history.

Results and discussion

Crystal structure and hydrogen desorption properties

Fig. 1 shows XRD patterns of investigated hydrogen storage alloys. The results indicated that the alloys are all single-phase alloys with hexagonal $CaCu_5$ type structure, though intensities of the characteristic peaks are slightly different from each other.

The crystallographic data, including refined unit cell parameters and unit cell volumes are summarized in Table 1. With the increase of metals with larger atomic radius such as Al and Cr crystal lattice slightly increases, whereas Nd with smaller atomic radius than La reduces unit cell parameters. Anisotropy (c/a ratio) stays almost unchanged.

Fig. 2 shows Pressure-Concentration-Temperature (PCT) isotherms of hydrogen desorption for La-, Nd- and Cr-alloys at room temperature. Equilibrium hydrogen desorption pressures are in a range of 0.005–0.01 MPa and show presence of a rather flat plateau. The highest hydrogen capacity of 1.23 wt% is observed for La-alloy. Partial substitution of La and Ni by Nd and Cr, respectively, slightly decreases gravimetric hydrogen concentration. The thermodynamic parameters of hydrogen desorption – enthalpy (ΔH) and entropy (ΔS) changes are calculated from PCT-isotherms at different temperatures using van't Hoff equation:

$$RlnP = \frac{\Delta H}{T} + \Delta S \quad (1)$$

where, R is a universal gas constant, P is the equilibrium hydrogen pressure, ΔH is the enthalpy change, T is the temperature and ΔS is the entropy change. Obtained thermodynamic values and hydrogen weight concentration are also listed in Table 1. All the investigated alloys are quite stable with ΔH of hydrogen desorption about 36–38 kJ/mol H_2.

Electrochemical properties

All the investigated alloys rapidly reached their maximum discharge capacity during the first 3–5 charge-discharge

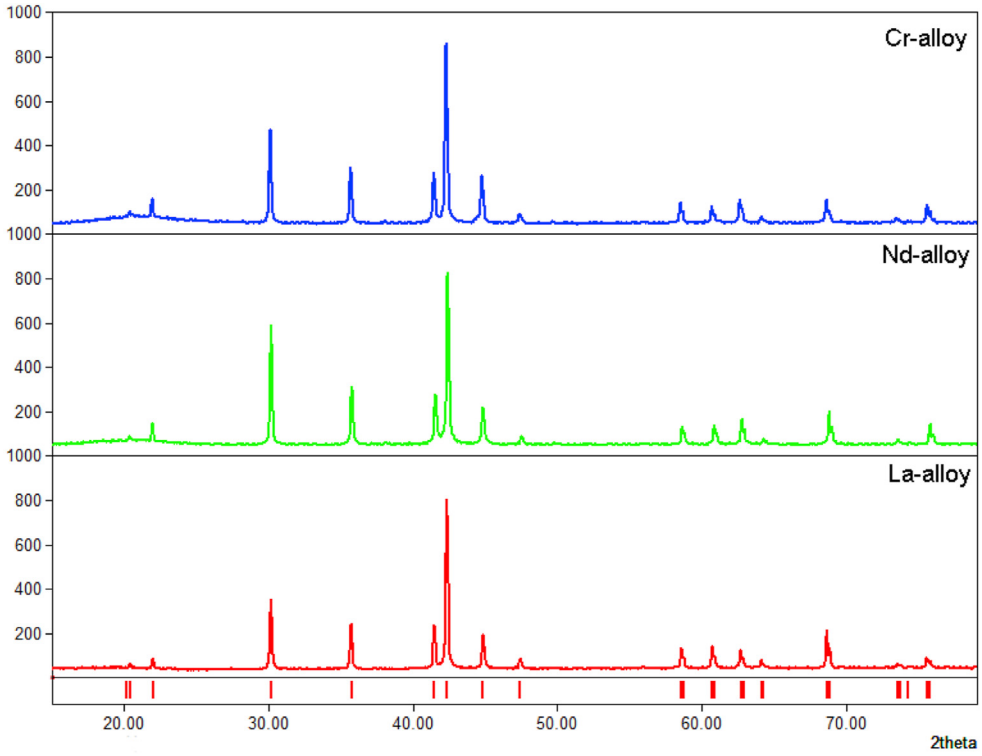

Fig. 1 – XRD patterns of AB_5 metal hydride alloys.

Table 1 – Crystal structure and hydrogen storage properties of AB_5 alloys.

Alloy	Unit cell parameters				Hydrogen content at 0.1 MPa, wt.%	ΔH_{des}, kJ/mol	ΔS_{des}, J/mol K
	a, Å	*c*, Å	*c*/*a*	V, Å^3			
La-alloy	5.029	4.042	0.804	88.5	1.23	36.8	103.8
Nd-alloy	5.013	4.038	0.806	87.9	1.16	36.0	105.6
Cr-alloy	5.027	4.045	0.805	88.5	1.07	38.1	104.5

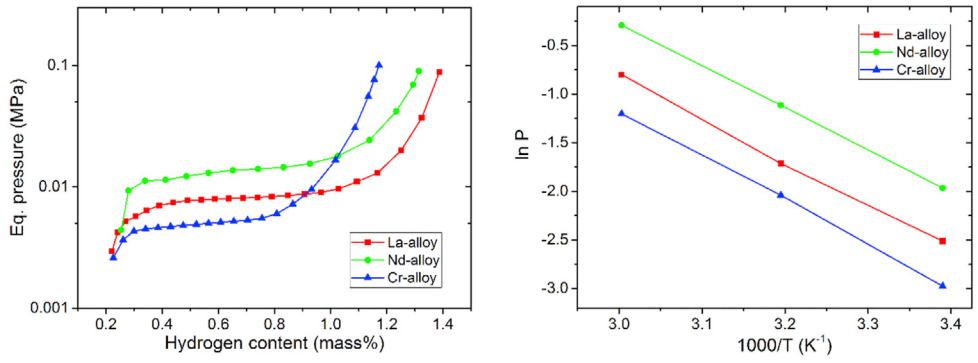

Fig. 2 – PCT isotherms of hydrogen desorption for annealed AB_5 alloys and van't Hoff plot.

cycles. The maximum discharge capacity is 321.1 mA h/g (10th cycle) for La-alloy during the activation at a charge-discharge current density of 100 mA/g (Fig. 3a). Nd- and Cr-alloys show lower maximum discharge capacities of 307.7 and 290.1 mA h/g, respectively. The results show the same dependence with the gas-phase results. Substitution La for Nd and Ni for Cr reduces both hydrogen storage and electrochemical capacities of metal hydrides. All the metal hydride electrodes have flat and broad plateau with an equilibrium potential of 0.87–0.9 V. A small reduction of equilibrium potential for Cr-alloy is observed. It is known that the discharge potential of the alloy electrode is associated with the surface activity, the electrolyte concentration and the internal resistance of the alloy electrode [57]. Ni is an

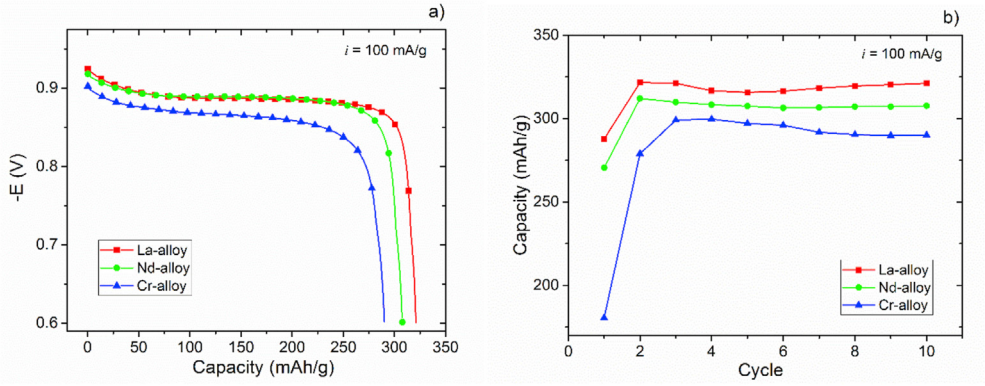

Fig. 3 – Maximum discharge capacity (a) and activation performance of the AB_5 alloys (b).

excellent catalyst due to formation of metallic clusters during activation, thus, reduction of Ni in alloy composition could result in decrease of the surface catalytic ability. It appears that substitution of Cr in the alloy deteriorates the surface activity of the electrode and thereby results in a lower value of the discharge potential.

The experimental results of electrochemical properties of investigated alloys in comparison with available data from literature are collected and summarized in Table 2. Obviously, it is difficult to compare electrochemical data from different researches because of a great difference in alloy preparation technique, annealing treatment conditions, metal hydride electrode fabrication, electrode activation and electrochemical measurement conditions. Both high-Co and low-Co containing metal hydride alloys show quite similar maximum discharge capacity around 300–330 mA h/g at 60 mA/g, and little smaller values at 100 mA/g.

High-rate dischargeability (HRD) of metal hydride electrode is one of the key characteristics for the development of Ni-MH batteries. The electrochemical reaction in metal hydride electrodes is associated with the processes of mass transfer, charge transfer and hydrogen diffusion. Charge transfer on the catalytic surface and hydrogen diffusion in the bulk occur simultaneously and both processes are limiting the electrode reactions [5,15]. HRD shows retention of discharge capacity during operation at high current densities.

High-rate dischargeability investigations show good performance for the alloys (Fig. 4). Cut-off potential for high rate dischargeability is setted to −0.6 V. The maximum discharge capacity at 1000 mA/g is achieved for La-alloy. The discharge capacity reaches 288.2 mA h/g and corresponds to 89.3% of the initial capacity. Nd-alloy and Cr-alloy show lower HRD performance and discharge capacities reach 244.4 (76.3%) and 222.1 (77.5%) mAh/g at 1000 mA/g, respectively. At low current

Table 2 – Electrochemical properties of AB_5 metal hydride alloys.

Alloy composition	Activation charge/discharge current density, mA/g	Maximum discharge capacity C_{max}, mAh/g	High rate discharge ability	Capacity retention at 1C, S_n	Hydrogen diffusion coefficient D, cm^2/s	Ref.
High-Co metal hydride alloys						
$La_{0.78}Ce_{0.22}Ni_{3.73}Mn_{0.3}Al_{0.17}Fe_{0.2}Co_{0.6}$	60/60	323	$HRD_{600} = 72.3\%$	$S_{150} = 79.6$	1.32×10^{-11}	[41]
$La_{0.6}Ce_{0.4}Ni_{3.45}Co_{0.75}Mn_{0.7}Al_{0.1}$	60/60	331	$HRD_{1200} \approx 68\%$	$S_{100} = 81.8\%$[a]	2.72×10^{-11}	[63]
$La_{0.78}Ce_{0.22}Ni_{3.8}Co_{0.6}Mn_{0.6}$	60/60	346.2	$HRD_{1500} = 39.4\%$	$S_{100} = 63.9\%$	1.79×10^{-11}	[32]
$MmNi_{3.7}Co_{0.7}Mn_{0.3}Al_{0.3}$	60/60	318.2	$HRD_{1500} = 52.9\%$	$S_{50} = 90.1\%$	1.83×10^{-11}	[33]
Low-Co metal hydride alloys						
$LaNi_{4.2}Co_{0.3}Mn_{0.3}Al_{0.2}$	60/60	330.4	$HRD_{900} = 78.2\%$	$S_{50} \approx 82\%$[a]	–	[38]
$LaNi_{3.55}Co_{0.15}Mn_{0.35}Al_{0.15}Cu_{0.75}(V_{0.81}Fe_{0.19})_{0.05}$	60/60	330.3	$HRD_{1200} = 58.5\%$	$S_{100} = 84.3\%$[a]	1.36×10^{-10}	[47]
$LaNi_{4.5}Co_{0.25}Al_{0.25}$	60/60	313.3	$HRD_{1800} = 70.2\%$	$S_{50} = 86.2\%$[a]	–	[64]
$LaNi_{4.3}Co_{0.4}Al_{0.3}$	185/100	310	$HRD_{600} \approx 32\%$	–	8.05×10^{-11}	[62]
$La_{0.6}Ce_{0.3}Nd_{0.05}Pr_{0.05}Ni_{3.9}Co_{0.4}Mn_{0.4}Al_{0.3}$	72/72	349	$HRD_{1440} = 59.9\%$	$S_{100} = 89.1\%$[a]	1.77×10^{-10}	[42]
$La_{0.8}Ce_{0.2}Ni_4Co_{0.4}Mn_{0.3}Al_{0.3}$ (La-alloy)	100/100	321.1	$HRD_{1000} = 89.3\%$	$S_{100} = 63.9\%$	6.9×10^{-13}[b]	This work
$La_{0.6}Ce_{0.2}Nd_{0.2}Ni_4Co_{0.4}Mn_{0.3}Al_{0.3}$ (Nd-alloy)	100/100	307.7	$HRD_{1000} = 76.3\%$	$S_{100} = 92.2\%$	3.7×10^{-13}[b]	This work
$La_{0.6}Ce_{0.2}Nd_{0.2}Ni_{3.8}Co_{0.4}Mn_{0.3}Al_{0.3}Cr_{0.2}$ (Cr-alloy)	100/100	290.1	$HRD_{1000} = 77.5\%$	$S_{100} = 77.3\%$	2.4×10^{-13}[b]	This work

[a] Cycling stability tests were performed at activation conditions.
[b] Hydrogen diffusion coefficients are measured at 100% SOC.

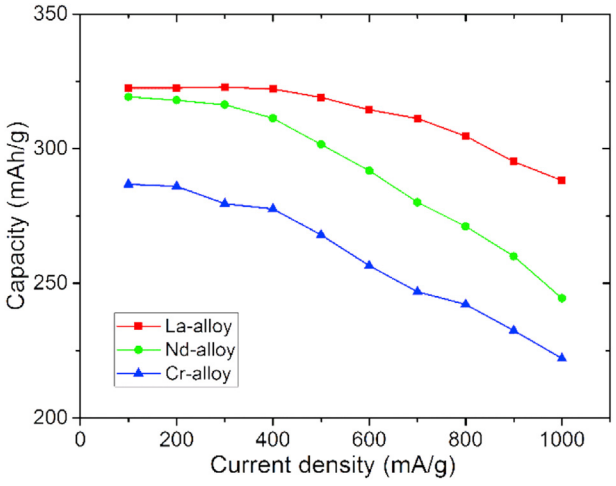

Fig. 4 – High-rate dischargeability of AB_5 metal hydride electrodes.

densities charge transfer, which determines the plateau width of the equilibrium potential, prevails over hydrogen diffusion. At high current densities, the rate-determining factor is hydrogen diffusion from the bulk to the electrode surface. High-rate dischargeability of Nd-alloy decreases faster than for La-alloy that well agreed with crystal structure parameters of the alloys.

Cycle stability of prepared metal hydride electrodes are investigated at charge-discharge current density of 300 mA/g (1C) during 100 cycles (see Fig. 5). Some incubation period to reach maximum discharge capacity during cycling tests is observed for all three metal hydride electrodes. The best cyclic performance is obtained for Nd-alloy. Capacity retention after 100 cycles reaches 280.5 mA h/g (92.2% of initial capacity at 300 mA/g). Capacity retention for La-alloy and Cr-alloy are quite lower 202.3 mA h/g (63.9%) and 236.3 mA h/g (77.3%). The main reason of discharge capacity degradation during cycling experiments is mechanical stability of prepared metal hydride electrode tablets. In cyclic experiments a gradual destruction

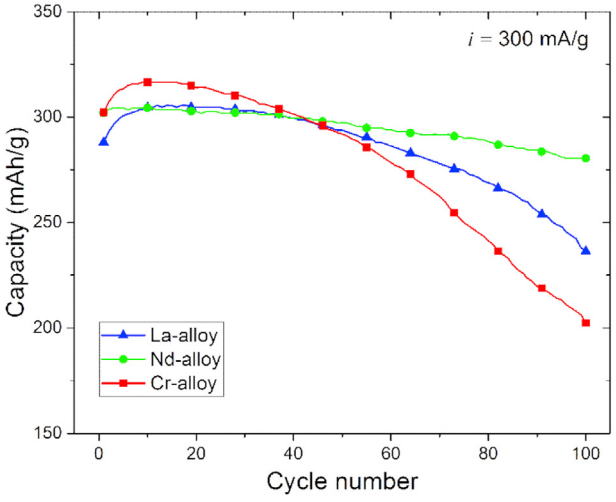

Fig. 5 – Cycling stability of AB_5 metal hydride alloys at current density of 300 mA/g.

of the tablet and the deposition of the powder at the bottom of the electrochemical cell is observed.

Hydrogen diffusion from the surface to bulk during hydrogen sorption is measured by potentiostatic intermittent titration technique (PITT). Current transients at low amplitude (20 mV) are measured in the potential range from −0.84 V to −0.98 V (Fig. 6a).

Each potential is applied until constant current is achieved. Experimental curves plotted $It^{1/2}$ vs log t coordinates are time invariant and should provide a horizontal section at short time domains, which corresponds to a typical Cottrellian behavior of diffusion [52]. It is assumed that the deviation of the $It^{1/2}$ vs log t curves from ideal conditions is because of the action of resistances in the electrochemical system that are not related to diffusion in the solid (for example, charge transfer and surface resistance at the interface), which impede the expected Cottrell behavior at short time domains. To calculate the effective hydrogen diffusion coefficient, we use the following equation [55,56]:

$$\frac{1}{I\sqrt{t}} = \frac{R_{\sum}}{\Delta E\sqrt{t}} + \frac{l\sqrt{\pi}}{\Delta Q\sqrt{D}} \quad (2)$$

where $R_{\sum}$ - sum of all non-diffusion resistances, ΔQ – integral capacity of electrode at given potential, D – diffusion coefficient, l – diffusion path length.

Linear dependence of experimental data on $It^{1/2}$ vs $1/t^{1/2}$ plot makes possible to calculate hydrogen diffusion coefficient for each potential step using Eq. (2). Diffusion path length is assumed to be a half of mean particle diameter and equals 25 μm. There is a negligible charge capacity change at low potentials under 0.88 V, which corresponds to less than 1% of total charge (Fig. 6b). On the other hand, potential step 0.98 V relates to overcharge process. In order to accurate calculation of hydrogen diffusion coefficient, we exclude first and last potential steps from fitting analysis. Fig. 7 shows a dependence of effective hydrogen diffusion coefficient from state of charge (SOC) of the metal hydride electrode in the potential range −0.88 to −0.96 V.

The maximum of hydrogen diffusion coefficients are reached at the beginning of the sorption process at low state of charge, which corresponds to α-solid solution region. As SOC increases hydrogen diffusion coefficients becomes lower decreasing to $2.4–6.9\cdot10^{-13}$ cm^2/s, because of saturation of β-hydride phase. Such behavior of hydrogen diffusion also noted for AB_3 [24,55] and AB_2 [56] type metal hydride electrodes and assumed to be typical for hydride forming alloys [58]. Hydrogen diffusion kinetics slightly reduces from La-alloy to Cr-alloy in a whole measured region. Cr-alloy with lower surface catalytic activity shows lower hydrogen diffusion kinetics through hydrogen sorption. After 50% SOC, which corresponds to mid of equilibrium plateau, hydrogen diffusion coefficient becomes almost constant. A similar dependence of hydrogen diffusion coefficient from depth of discharge are obtained modified from Warburg impedance [59] and cyclic voltammetry [60].

The hydrogen diffusion coefficients at low state of charge are in good agreement with those obtained from literature. As usual, the hydrogen diffusion coefficient in the intermetallics is measured by constant potential step methods on the

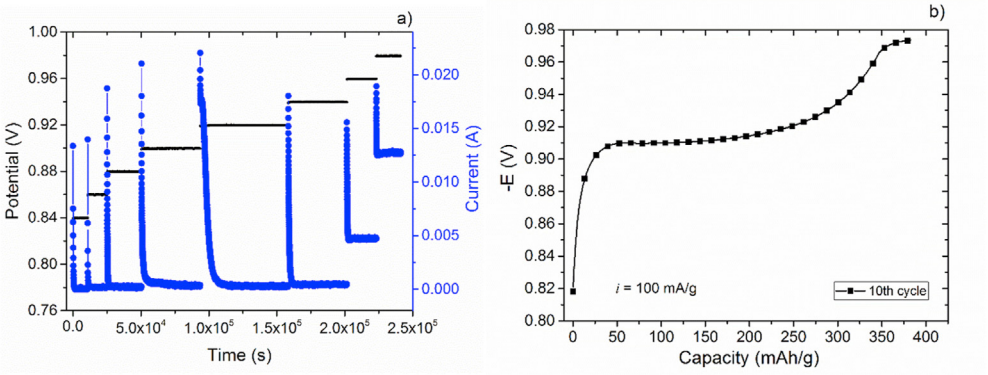

Fig. 6 – Time dependence of currents as related to applied potentials (a) and charge curve of 10th activation cycle for La-alloy (b).

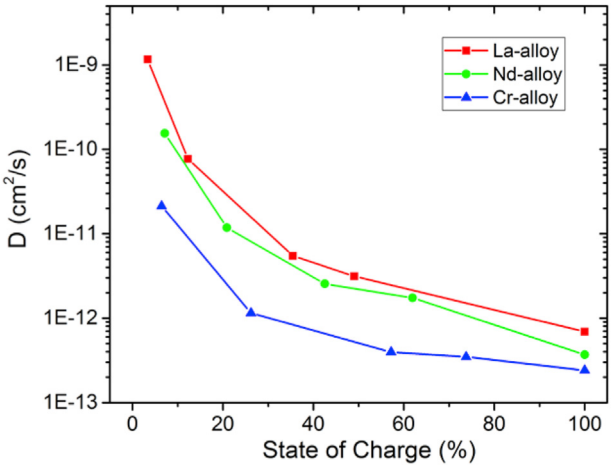

Fig. 7 – Hydrogen diffusion coefficient *vs* state of charge (SOC) of metal hydride electrodes.

discharge and calculated according to Zheng model [61] by fitting the slope of the linear portion of response curves [32,33,42,47,62,63]. The linear portions, from which hydrogen diffusion is calculated, relate to the end of discharge, which also corresponds α-solid solution region. Therefore, hydrogen diffusion coefficients from PITT are in good agreement with those obtained from constant potential step method. The hydrogen diffusion coefficients corresponding to saturated β-region during charging are 2–3 orders lower, than those obtained for discharge process by potential step methods, which corresponds to higher diffusion resistance during charging rather than discharging.

Conclusions

Three different annealed low Co AB_5-type intermetallic compounds have been investigated in terms of phase structure, hydrogen storage and electrochemical properties. The XRD results indicated that annealed alloys are all single-phase alloys with $CaCu_5$ type structure. The maximum of both hydrogen content and discharge capacity is obtained for La-alloy 1.23 wt%H_2 and 321.1 mA h/g, respectively. All the investigated alloys are quiet stable with ΔH of hydrogen desorption about 36–38 kJ/mol H_2. Cycle life of alloy electrode has been improved by partial substitution of La for Nd and Ni for Cr. The highest capacity retention of 92.2% after 100 charge/discharge cycles at 1C has been observed for Nd-alloy. The hydrogen diffusion coefficient measured by PITT is higher at the start of charging process and dramatically reduces by 2–3 order of magnitude with saturation of β-hydride. The highest value 6.9×10^{-13} cm^2/s is observed for La alloy at 100% SOC. Partial substitution La for Nd and Cr for Ni in low-Co AB_5 metal hydride alloys slightly reduces maximum discharge capacity, HRD performance and hydrogen diffusion kinetics. Low-Co alloys show good overall electrochemical properties compared to high-Co alloys and might be perspective materials for various electrochemical applications.

Declaration of competing interest

The authors declare that they have no known competing financial interests or personal relationships that could have appeared to influence the work reported in this paper.

Acknowledgement

This work was partially supported by grant 18-08-01497 from the Russian Foundation for Basic Research. Authors would like to thank members of Laboratory for Hydrogen Energy Technologies of JIHT RAS and members of Laboratory of Energocapacious and Catalytically Active Substances of Moscow State University for discussion, useful advices and practical help in the research.

REFERENCES

[1] Rusman NAA, Dahari M. A review on the current progress of metal hydrides material for solid-state hydrogen storage

applications. Int J Hydrogen Energy 2016;41:12108–26. https://doi.org/10.1016/j.ijhydene.2016.05.244.
[2] Gary S. A panoramic overview of hydrogen storage alloys from a gas reaction point of view. J Alloys Compd 1999;293–295:877–88. https://doi.org/10.1016/s0925-8388(99)00384-9.
[3] Lototskyy MV, Yartys VA, Pollet BG, Bowman Jr RC. Metal hydride hydrogen compressors: a review. Int J Hydrogen Energy 2014;39:5818–51. https://doi.org/10.1016/j.ijhydene.2014.01.158.
[4] Manickam K, Mistry P, Walker G, Grant D, Buckley CE, Humphries TD, et al. Future perspectives of thermal energy storage with metal hydrides. Int J Hydrogen Energy 2019;44:7738–45. https://doi.org/10.1016/j.ijhydene.2018.12.011.
[5] Ouyang L, Huang J, Wang H, Liu J, Zhu M. Progress of hydrogen storage alloys for Ni-MH rechargeable power batteries in electric vehicles: a review. Mater Chem Phys 2017;200:164–78. https://doi.org/10.1016/j.matchemphys.2017.07.002.
[6] Young K-h, Nei J. The current status of hydrogen storage alloy development for electrochemical applications. Materials 2013;6:4574.
[7] Hu W-K, Noréus D. Metal hydrides as bi-functional catalysts for hydrogen generation and oxidation in reversible MH-air fuel cells. Electrochem Commun 2009;11:2212–5. https://doi.org/10.1016/j.elecom.2009.09.033.
[8] Chartouni D, Kuriyama N, Kiyobayashi T, Chen J. Metal hydride fuel cell with intrinsic capacity. Int J Hydrogen Energy 2002;27:945–52. https://doi.org/10.1016/S0360-3199(01)00186-0.
[9] Folonari C, Iemmi G, Manfredi F, Rolle A. Metal hydride fuel cells: a feasibility study and perspectives for vehicular applications. J Less Common Met 1980;74:371–8. https://doi.org/10.1016/0022-5088(80)90175-7.
[10] Lemmon JP. Energy: reimagine fuel cells. Nature 2015;525:447–9. https://doi.org/10.1038/525447a.
[11] Hu W-K, Noréus D. Lab-size rechargeable metal hydride–air cells. J Power Sources 2010;195:5810–3. https://doi.org/10.1016/j.jpowsour.2010.03.086.
[12] Fok K. Metal hydride fuel cells, A new and practical approach for backup and emergency power applications. In: INTELEC 06 - twenty-eighth international telecommunications energy conference; 2006. p. 1–6. https://doi.org/10.1109/INTLEC.2006.251656.
[13] Choi B, Panthi D, Nakoji M, Kabutomori T, Tsutsumi K, Tsutsumi A. Novel hydrogen production and power generation system using metal hydride. Int J Hydrogen Energy 2015;40:6197–206. https://doi.org/10.1016/j.ijhydene.2015.03.029.
[14] Liu Y, Pan H, Gao M, Wang Q. Advanced hydrogen storage alloys for Ni/MH rechargeable batteries. J Mater Chem 2011;21:4743–55. https://doi.org/10.1039/C0JM01921F.
[15] Tliha M, Khaldi C, Boussami S, Fenineche N, El-Kedim O, Mathlouthi H, et al. Kinetic and thermodynamic studies of hydrogen storage alloys as negative electrode materials for Ni/MH batteries: a review. J Solid State Electrochem 2014;18:577–93. https://doi.org/10.1007/s10008-013-2300-3.
[16] Kleperis J, Wójcik G, Czerwinski A, Skowronski J, Kopczyk M, Beltowska-Brzezinska M. Electrochemical behavior of metal hydrides. J Solid State Electrochem 2001;5:229–49. https://doi.org/10.1007/s100080000149.
[17] Feng F, Geng M, Northwood DO. Electrochemical behaviour of intermetallic-based metal hydrides used in Ni/metal hydride (MH) batteries: a review. Int J Hydrogen Energy 2001;26:725–34. https://doi.org/10.1016/S0360-3199(00)00127-0.
[18] Hong K. The development of hydrogen storage alloys and the progress of nickel hydride batteries. J Alloys Compd 2001;321:307–13. https://doi.org/10.1016/S0925-8388(01)00957-4.
[19] Petrii OA, Levin EE. Hydrogen-accumulating materials in electrochemical systems. Russ J Gen Chem 2007;77:790–6. https://doi.org/10.1134/s1070363207040408.
[20] Liu Y, Cao Y, Huang L, Gao M, Pan H. Rare earth–Mg–Ni-based hydrogen storage alloys as negative electrode materials for Ni/MH batteries. J Alloys Compd 2011;509:675–86. https://doi.org/10.1016/j.jallcom.2010.08.157.
[21] Takasaki T, Nishimura K, Saito M, Fukunaga H, Iwaki T, Sakai T. Cobalt-free nickel–metal hydride battery for industrial applications. J Alloys Compd 2013;580:S378–81. https://doi.org/10.1016/j.jallcom.2013.01.092.
[22] Young K-H, Chang S, Lin X. C14 laves phase metal hydride alloys for Ni/MH batteries applications. Batteries 2017;3:27.
[23] Yan H, Xiong W, Wang L, Li B, Li J, Zhao X. Investigations on AB3-, A2B7- and A5B19-type LaYNi system hydrogen storage alloys. Int J Hydrogen Energy 2017;42:2257–64. https://doi.org/10.1016/j.ijhydene.2016.09.049.
[24] Volodin AA, Wan C, Denys RV, Tsirlina GA, Tarasov BP, Fichtner M, et al. Phase-structural transformations in a metal hydride battery anode La1.5Nd0.5MgNi9 alloy and its electrochemical performance. Int J Hydrogen Energy 2016;41:9954–67. https://doi.org/10.1016/j.ijhydene.2016.01.089.
[25] Verbovyts'kyi YV, Zavalii IY. New metal-hydride electrode materials based on R1–x Mg x Ni3–4 alloys for chemical current sources. Mater Sci 2016;51:443–56. https://doi.org/10.1007/s11003-016-9861-0.
[26] Denys RV, Yartys VA, Webb CJ. Hydrogen in La2MgNi9D13: the role of magnesium. Inorg Chem 2012;51:4231–8. https://doi.org/10.1021/ic202705u.
[27] Zhang Y-h, Cai Y, Zhao C, Zhai T-t, Zhang G-f, Zhao D-l. Electrochemical performances of the as-melt La0.75−xMxMg0.25Ni3.2Co0.2Al0.1 (M = Pr, Zr; x = 0, 0.2) alloys applied to Ni/metal hydride (MH) battery. Int J Hydrogen Energy 2012;37:14590–7. https://doi.org/10.1016/j.ijhydene.2012.07.020.
[28] Binnemans K, Jones PT, Blanpain B, Van Gerven T, Yang Y, Walton A, et al. Recycling of rare earths: a critical review. J Clean Prod 2013;51:1–22. https://doi.org/10.1016/j.jclepro.2012.12.037.
[29] Andrievski RA, Tarasov BP, Korobov II, Mozgina NG, Shilkin SP. Hydrogen absorption and electrocatalytic properties of ultrafine LaNi5 powders. Int J Hydrogen Energy 1996;21:949–54. https://doi.org/10.1016/S0360-3199(96)00074-2.
[30] Tarasov BP. Metal-hydride accumulators and generators of hydrogen for feeding fuel cells. Int J Hydrogen Energy 2011;36:1196–9. https://doi.org/10.1016/j.ijhydene.2010.07.002.
[31] Liu W, Aguey-Zinsou K-F. Low temperature synthesis of LaNi5 nanoparticles for hydrogen storage. Int J Hydrogen Energy 2016;41:1679–87. https://doi.org/10.1016/j.ijhydene.2015.10.128.
[32] Zhou W, Zhu D, Tang Z, Wu C, Huang L, Ma Z, et al. Improvement in low-temperature and instantaneous high-rate output performance of Al-free AB5-type hydrogen storage alloy for negative electrode in Ni/MH battery: effect of thermodynamic and kinetic regulation via partial Mn substituting. J Power Sources 2017;343:11–21. https://doi.org/10.1016/j.jpowsour.2017.01.023.
[33] Zhou W, Tang Z, Zhu D, Ma Z, Wu C, Huang L, et al. Low-temperature and instantaneous high-rate output performance of AB5-type hydrogen storage alloy with duplex surface hot-alkali treatment. J Alloys Compd 2017;692:364–74. https://doi.org/10.1016/j.jallcom.2016.08.292.

[34] Yang S, Han S, Song J, Li Y. Influences of molybdenum substitution for cobalt on the phase structure and electrochemical kinetic properties of AB5-type hydrogen storage alloys. J Rare Earths 2011;29:692–7. https://doi.org/10.1016/S1002-0721(10)60524-8.
[35] Wei X, Liu S, Dong H, Zhang P, Liu Y, Zhu J, et al. Microstructures and electrochemical properties of Co-free AB5-type hydrogen storage alloys through substitution of Ni by Fe. Electrochim Acta 2007;52:2423–8. https://doi.org/10.1016/j.electacta.2006.08.067.
[36] Vivet S, Joubert JM, Knosp B, Percheron-Guégan A. Effects of cobalt replacement by nickel, manganese, aluminium and iron on the crystallographic and electrochemical properties of AB5-type alloys. J Alloys Compd 2003;356–357:779–83. https://doi.org/10.1016/S0925-8388(03)00087-2.
[37] Råde I, Andersson BA. Requirement for metals of electric vehicle batteries. J Power Sources 2001;93:55–71. https://doi.org/10.1016/S0378-7753(00)00547-4.
[38] Balogun M-S, Wang Z-m, Chen H-x, Deng J-q, Yao Q-r, Zhou H-y. Effect of Al content on structure and electrochemical properties of LaNi4.4 – xCo0.3Mn0.3Alx hydrogen storage alloys. Int J Hydrogen Energy 2013;38:10926–31. https://doi.org/10.1016/j.ijhydene.2013.02.139.
[39] Yang S, Han S, Li Y, Liu J. Study on the microstructure and electrochemical kinetic properties of MmNi4.50–xMnxCo0.45Al0.30 (0.25≤x≤0.45) hydrogen storage alloys. Mater Sci Eng, B 2013;178:39–44. https://doi.org/10.1016/j.mseb.2012.10.010.
[40] Liu B-z, Li A-m, Fan Y-p, Hu M-j, Zhang B-q. Phase structure and electrochemical properties of La0.7Ce0.3Ni3.75Mn0.35Al0.15Cu0.75-xFex hydrogen storage alloys. Trans Nonferrous Metals Soc China 2012;22:2730–5. https://doi.org/10.1016/S1003-6326(11)61525-2.
[41] Dongliang C, Chenglin Z, Zhewen M, Fei Y, Yucheng W, Ding Z, et al. Improvement in high-temperature performance of Co-free high-Fe AB5-type hydrogen storage alloys. Int J Hydrogen Energy 2012;37:12375–83. https://doi.org/10.1016/j.ijhydene.2012.05.147.
[42] Zhang W, Han S, Hao J, Li Y, Bai T, Zhang J. Study on kinetics and electrochemical properties of low-Co AB5-type alloys for high-power Ni/MH battery. Electrochim Acta 2009;54:1383–7. https://doi.org/10.1016/j.electacta.2008.09.019.
[43] Balogun M-S, Wang Z, Zhang H, Yao Q, Deng J, Zhou H. Effect of high and low temperature on the electrochemical performance of LaNi4.4–xCo0.3Mn0.3Alx hydrogen storage alloys. J Alloys Compd 2013;579:438–43. https://doi.org/10.1016/j.jallcom.2013.06.031.
[44] Peng X, Liu B, Fan Y, Ji L, Zhang B, Zhang Z. Microstructures and electrochemical characteristics of La0.7Ce0.3Ni4.2Mn0.9–xCu0.37(V0.81Fe0.19)x hydrogen storage alloys. Electrochim Acta 2013;93:207–12. https://doi.org/10.1016/j.electacta.2013.01.110.
[45] Liu B, Hu M, Li A, Ji L, Zhang B, Zhu X. Microstructure and electrochemical characteristics of La0.7Ce0.3Ni3.75Mn0.35Al0.15Cu0.75-x(V0.81Fe0.19)x hydrogen storage alloys. J Rare Earths 2012;30:769–74. https://doi.org/10.1016/S1002-0721(12)60127-6.
[46] Liu B, Hu M, Zhou Y, Li A, Ji L, Fan Y, et al. Microstructures and electrochemical characteristics of La0.7Ce0.3Ni3.75–xCu0.75Mn0.35Al0.15(V0.81Fe0.19)x (x=0–0.20) hydrogen storage alloys. J Alloys Compd 2012;544:105–10. https://doi.org/10.1016/j.jallcom.2012.07.141.
[47] Liu B, Peng X, Fan Y, Ji L, Zhang B, Zhang Z. Microstructures and electrochemical properties of LaNi3.55Co0.2xMn0.35Al0.15Cu0.75(V0.81Fe0.19)x hydrogen storage alloys. Int J Electrochem Sci 2012;7:11966–77.
[48] Zhou Z, Song Y, Cui S, Huang C, Qian W, Lin C, et al. Effect of annealing treatment on structure and electrochemical performance of quenched MmNi4.2Co0.3Mn0.4Al0.3Mg0.03 hydrogen storage alloy. J Alloys Compd 2010;501:47–53. https://doi.org/10.1016/j.jallcom.2010.04.026.
[49] Shen Y, Peng F, Kontos S, Noréus D. Improved NiMH performance by a surface treatment that creates magnetic Ni-clusters. Int J Hydrogen Energy 2016;41:9933–8. https://doi.org/10.1016/j.ijhydene.2016.01.145.
[50] Ye Z, Noréus D. Metal hydride electrodes: the importance of surface area. J Alloys Compd 2016;664:59–64. https://doi.org/10.1016/j.jallcom.2015.12.170.
[51] Yang S, Liu Z, Han S, Zhang W, Song J. Effects of annealing treatment on the microstructure and electrochemical properties of low-Co hydrogen storage alloys containing Cu and Fe. Rare Met 2011;30:464. https://doi.org/10.1007/s12598-011-0414-2.
[52] Aurbach D, Levi MD, Levi E. A review on the solid-state ionics of electrochemical intercalation processes: how to interpret properly their electrochemical response. Solid State Ionics 2008;179:742–51. https://doi.org/10.1016/j.ssi.2007.12.070.
[53] Levi MD, Markevich E, Aurbach D. The effect of slow interfacial kinetics on the chronoamperometric response of composite lithiated graphite electrodes and on the calculation of the chemical diffusion coefficient of Li ions in graphite. J Phys Chem B 2005;109:7420–7. https://doi.org/10.1021/jp0441902.
[54] Levi MD, Demadrille R, Pron A, Vorotyntsev MA, Gofer Y, Aurbach D. Application of a novel refinement method for accurate determination of chemical diffusion coefficients in electroactive materials by potential step technique. J Electrochem Soc 2005;152:E61. https://doi.org/10.1149/1.1851033.
[55] Volodin AA, Denys RV, Tsirlina GA, Tarasov BP, Fichtner M, Yartys VA. Hydrogen diffusion in La1.5Nd0.5MgNi9 alloy electrodes of the Ni/MH battery. J Alloys Compd 2015;645:S288–91. https://doi.org/10.1016/j.jallcom.2014.12.201.
[56] Volodin AA, Denys RV, Wan C, Wijayanti ID, Suwarno, Tarasov BP, et al. Study of hydrogen storage and electrochemical properties of AB2-type Ti0.15Zr0.85La0.03Ni1.2Mn0.7V0.12Fe0.12 alloy. J Alloys Compd 2019;793:564–75. https://doi.org/10.1016/j.jallcom.2019.03.134.
[57] Shi S, Ouyang C, Lei M. Crystal structure and electrochemical characteristics of non-AB5 type La–Ni system alloys. J Power Sources 2007;164:911–5. https://doi.org/10.1016/j.jpowsour.2006.09.113.
[58] Young K, Chao B, Pawlik D, Shen HT. Transmission electron microscope studies in the surface oxide on the La-containing AB2 metal hydride alloy. J Alloys Compd 2016;672:356–65. https://doi.org/10.1016/j.jallcom.2016.02.182.
[59] Yuan X, Xu N. Determination of hydrogen diffusion coefficient in metal hydride electrode by modified Warburg impedance. J Alloys Compd 2001;329:115–20. https://doi.org/10.1016/S0925-8388(01)01569-9.
[60] Yuan X, Xu N. Determination of hydrogen diffusion coefficient in metal hydride electrode by cyclic voltammetry. J Alloys Compd 2001;316:113–7. https://doi.org/10.1016/S0925-8388(00)01287-1.
[61] Zheng G. Electrochemical determination of the diffusion coefficient of hydrogen through an LaNi[sub 4.25]Al[sub 0.75] electrode in alkaline aqueous solution. J Electrochem Soc 1995;142:2695. https://doi.org/10.1149/1.2050076.

[62] Giza K. Electrochemical studies of LaNi4.3Co0.4Al0.3 hydrogen storage alloy. Intermetallics 2013;34:128–31. https://doi.org/10.1016/j.intermet.2012.11.014.
[63] Lin J, Cheng Y, Liang F, Sun L, Yin D, Wu Y, et al. High temperature performance of La0.6Ce0.4Ni3.45Co0.75Mn0.7Al0.1 hydrogen storage alloy for nickel/metal hydride batteries. Int J Hydrogen Energy 2014;39:13231–9. https://doi.org/10.1016/j.ijhydene.2014.06.112.
[64] Yao QR, Zhou HY, Wang ZM, Pan SK, Rao GH. Electrochemical properties of the LaNi4.5Co0.25Al0.25 hydrogen storage alloy in wide temperature range. J Alloys Compd 2014;606:81–5. https://doi.org/10.1016/j.jallcom.2014.04.026.